Journal of Natural Remedies
DOI: 10.18311/jnr/2026/56049

Research Article
eISSN: 2320-3358 | Vol 26(9), 2026 | pp. 2471-2491

Hepatic Protection against Anti-tubercular Drug-induced Hepatotoxicity with *Phyllanthus acidus* Bark Extract – *In Silico*, *In Vitro* and *In Vivo* Methods

Humaira Fatima[1,2], Rokeya Sultana[1*] and S. Roshan[1,2]

[1]Yenepoya Pharmacy College and Research Centre, Yenepoya (Deemed to be University), Mangalore - 575018, Karnataka, India; drrokeyasultana@yenepoya.edu.in

[2]Deccan School of Pharmacy, Osmania University, Hyderabad - 500001, Telangana, India

Abstract

Background: Drug-related liver injury is rising annually. Isoniazid (INH) and Rifampicin (RFP), used in tuberculosis, cause liver injury as side effects. Natural ingredients provide marked benefits in causing liver injury risk. *Phyllanthus acidus* (L.) Skeels (family: *Euphorbiaceae*), bark has shown hepatoprotective, antibacterial, and antioxidant activities. **Aim:** This research study was conducted to investigate the hepatic protection ability of *P. acidus* bark against isoniazid- and rifampicin-induced hepatotoxicity. **Methods:** This study included the total terpenoid, phenolic, and flavonoid content's quantitative estimations, antioxidant assays, GCMS method, molecular docking, XTT assay using HepG2 cell lines and also *in vivo* studies were conducted using isoniazid and rifampicin (50 mg/kg and 100 mg/kg *b.w,* respectively*),* 200 and 400 mg/kg *b.w* extract and silymarin 100 mg/kg *b.w*; serum parameters, inflammatory cytokines, and oxidative stress parameters, and histopathological studies were carried out. **Results:** The total terpenoid, phenolic and flavonoid contents were calculated as 39.00±1.00%, g/g, 28.13±0.005 mg GAE/g and 351.70±0.993 mg QE/g, respectively. The IC_{50} values for the DPPH, reducing power and nitric acid methods are found to be 216.41 ± 0.189, 191.65±0.142 and 85.25±0.107 µg/mL, respectively. GC-MS method revealed the presence of nine bioactive principles in the extract; upon molecular docking, Kauran-18-al, 17-(acetyloxy)-, (4.beta.)- has the nearest docking score to silymarin. ADME and toxicity prediction studies were also performed. In the XTT assay, the extract produced a dose-dependent curve, and IC_{50} values of the extract and Doxorubicin were obtained as 57.59 and 5.99µM respectively. In the *in vivo* studies, the high dose of extract improved the serum parameters, inflammatory cytokines and oxidative stress parameters compared to silymarin and the histomorphological characteristics of the liver were well protected from damage. **Conclusion:** *P. acidus* bark extract is beneficial for the protection of hepatic damage due to isoniazid and rifampicin-induced hepatotoxicity during antitubercular therapy.

Major Findings: *P. acidus* bark has shown promising therapeutic efficacy and could be included as an adjunct in the antitubercular therapy regimen as an effective hepatoprotective agent.

Keywords: HepG2 Cell Lines, Isoniazid, Rifampicin, *Phyllanthus acidus,* XTT Assay

(Article Chronicle: Article Received on: 03.05.2026; Revised on: 16.07.2026; Accepted on: 28.07.2026)

1. Introduction

Drug-induced hepatic damage occurs due to dietary adjuncts, drugs, and their adducts, and its frequency is spiking annually. It is the fifth main cause of fatality due to hepatic problems around the world; hence, drug-induced hepatic damage has earned significant recognition[1]. Regardless of prodigious advances in progressive medicine, the safeguard and cure of hepatic problems such as hepatocellular carcinoma, fibrosis, chronic hepatitis, and cirrhosis prevails major health concerns in the current world[2].

*Author for correspondence

The liver has a major function in metabolism, detoxification and further maintains hemostasis[3]. Tuberculosis continues to be a recurrent health issue in developing nations[4]. INH and RFP are the frontline therapies in tuberculosis. Alone or in combination, isoniazid and rifampicin lead to hepatic injury, causing hepatic failure, reckoning 5-22% of acute hepatic failure instances[5]. The occurrence of liver toxicity in India is 11.6%, in comparison with Western nations, where the prevalence is 4.3%[6]. Natural medicines have the features of multi-target, multi-level, and multifaceted overarching order and possess exceptional benefits in remedying symptoms of patient, decreasing the likelihood of hepatic damage, retarding the advancement of hepatic injury, and improving the body's potential to repair. In recent times, natural remedies have produced adequate protective activity against hepatic damage due to INH and RFP administrations[1].

Phyllanthus acidus (L.) Skeels (*Euphorbiaceae* family), popular as star gooseberry or harfarauri, is extensively distributed in India and various Asian countries[7]. *P. acidus* bark is traditionally used for itching, skin rashes[8], bronchial problems[9], purgative and emetic[10,11]. Phytochemical analyses of the bark have identified diterpenes, sesquiterpenes, triterpenes, and glycosides, which are the chief classes of active substances[12]. In the bark, phyllanthol, β-amyrin, and pentacyclic triterpenoids, sesquiterpenoids like Norbisabolane-type containing a spiroketal component, phyacidusin A and B, phllanthacidoid A1 and N1, and four novel norbisabolane-type sesquiterpenoids[13,14]. The bark is reported to have antioxidant, hepatoprotective, and antibacterial activities[15,16].

This investigation is devised to assess the hepatoprotective potential of the methanolic extract of *P. acidus* bark on isoniazid- and rifampicin-induced liver injury in rats, in comparison with the standard drug silymarin. For the validation of the study, chromatographic analysis, docking method, and *in vitro* methods were applied.

2. Material and Methods

2.1 Drugs and Chemicals

This investigation has utilised the following chemicals and kits: INH, RFP, and Silymarin, XTT reduction assay kit (Sigma-Aldrich, USA), blood-serum parameters kits (Erba, India), oxidative stress parameters (Sigma-Aldrich kits), and inflammatory cytokine parameters (ELISA kit) and other analytical-grade chemicals.

2.2 Collection, Authentication, Drying, and Size Reduction

Phyllanthus acidus bark was collected from the local area of Ranga Reddy district, Hyderabad, Telangana state and was authenticated by L. Rasingam, Scientist – 'E' and HoO, Botanical Survey of India, bearing the authentication no. BSI/DRC/2022-2023/identification/167. The bark was cleaned, dried in the shade, and ground to a fine powder.

2.3 Extraction

Dried powdered bark (250 g) was extracted by the Soxhlet method using methanol (1000 mL) till the powder was exhausted of phytoconstituents. The extract was then concentrated using a rotary vacuum evaporator at a temperature of 40- 60°C under vacuum and used for further studies.

2.4 Quantitative Estimations

2.4.1 Total Terpenoid Content

Two grams of bark powder were taken and soaked for 24 h using methanol. Filtered, and the filtrate was further extracted with petroleum ether. The residue collected was dried, weighed, and the total terpenoid content was estimated by using the formula[17].

$$\text{Total terpenoid content} = \frac{\textit{Final weight of the sample} - \textit{Initial weight of the extract}}{\textit{weight of the sample}} \times 100$$

2.4.2 Determination of Total Phenolics

For the estimation, 0.5 mL of bark extract or standard gallic acid solution of various concentrations was added to 2.5 mL of 10% Folin–Ciocalteu reagent and 2.5 mL of 7.5% Sodium carbonate solution and incubated for 25 min at 25°C, and the absorbances were recorded at 760 nm[18].

2.4.3 Determination of Total Flavonoids

1.0 mL of bark extract or standard of various concentrations was added with 3 mL methanol, 0.2 mL 1 M potassium acetate, 0.2 mL 10% $AlCl_3$, and 5.6 mL

of water, incubated for 25 min, and absorbances were observed at 420 nm[19].

2.5 *In Vitro* Determination of Antioxidant Activity

2.5.1 DPPH (1,1-Diphenyl-2-picrylhydrazyl) Radical Scavenging Assay

The standard and bark extract solutions (50-250 µg/mL) in methanol were prepared; then 1 mL of 0.135 mM DPPH methanolic solution was added, left in the dark for 30 min at room temperature, and absorbances were noted at 517 nm and % radical scavenging activity was calculated.

$$\textit{Radical scavenging activity (\%)} = (A_c\text{-}A_t/A_c) \text{ X } 100$$

Here, A_c and A_t are the absorbance values of the control and test/standard, respectively. IC_{50} was determined from the graph of the percentage radical scavenging activity of the standard and extract concentrations.

2.5.2 Reducing Power Assay

The standard and bark extract solutions (50-250 µg/mL) were prepared in methanol; 1 mL of distilled water was added with phosphate buffer (2.5 mL, 2 M, pH 6.6) and potassium ferricyanide (2.5 mL, 1%), incubated for 20 min at 50°C and 2.5 mL of 10% trichloroacetic acid was incorporated and centrifuged at 1500 rpm (10 min). 2.5 mL of the supernatant layer was added to 2.5 mL distilled water and 0.5 mL 0.1% $FeCl_3$. The absorbance values were recorded at 700 nm and % reducing power was estimated by:

$$\textit{Reducing power (\%)} = (A_c\text{-}A_t/A_c) \text{ X } 100$$

Here, A_c and A_t are the absorbance values of the control and test/standard, respectively. IC_{50} was determined from the graph of percentage radical scavenging activity, the standard and extract concentration.

2.5.3 Nitric Oxide Scavenging Assay

Methanol is used as a vehicle for the preparation of extract and standard solutions. 0.5 mL of 10 $mmolL^{-1}$ sodium nitroprusside in phosphate-buffered saline (pH 7.4) was added to the extract and standard solutions and incubated for 150 min (25°C). After 3 h, 0.5 mL of Griess reagent was added, and the mixture was incubated for 30 min, after which the absorbance at 546 nm was checked.

$$\textit{Nitric oxide scavenging (\%)} = (A_c\text{-}A_t/A_c) \text{ X } 100$$

Here, A_c and A_t are the absorbances of the control and test/standard, respectively. IC_{50} was determined from the graph of percentage radical scavenging activity, the standard and extract concentration[20].

2.6 Gas Chromatography-Mass Spectrometry (GC-MS) Analysis

The Clarus 680 GC with a fused silica column, Elite-5MS (5% biphenyl 95% dimethyl polysiloxane, 30 m × 0.25 mm ID × 250 µm df) and Helium gas at a 1 mL/min flow rate was utilised. A temperature of 260 °C was set at the injector during the analysis. 1 µL of bark extract was introduced, where a 60°C oven temperature was maintained for 2 min, then 300°C with a rate of 10°C/min for 6 min. The transfer line temperature of the mass detector was set at 230°C; the ion source temperature was maintained at 230°C; and for ionisation mode, electron impact was set at 70 eV, with a scan time of 0.2 s and a scan interval of 0.1 s. The fragmentation ranges from 40-600 Da. The spectra of the compounds were compared with the spectra of known compounds available in the database stored in the GC-MS NIST (2008) library[21].

2.7 Molecular Docking

PDB ID: 5HYK was chosen, which was fetched from the PDB, *i.e.*, Protein Data Bank. The protein preparation wizard panel processed the protein structure. An inactive protein site grid was produced by Glide v 9.1, receptor grid generation panel. Ligand preparation (LigPrep) was carried out using the OPLS 5 force field for geometric minimisation. The docking was performed by GLIDE's Ligand Docking Module. Initially, the Receptor Grid was chosen, then LigPrep was selected by opting for XP mode. The docking scores were examined in the project table. The ligand interlinkage diagram shows the protein and ligand interactions. Prime/MM-GBSA was employed to study the relative binding energy of specific ligands. The pv. maegz file from XP docking was utilised; also, the active sites of the protein were set up for self-correction up to a 5 Å ligand proximity[22].

2.8 XTT Cell Proliferation Assay

XTT assay was used to check the anti-proliferative activity of the bark extract in HepG2 cell lines. The assessment was conducted according to the procedure provided by the manufacturer (Sigma-Aldrich, USA). Each cell line, after reaching more than 80% confluency in each well, was treated for 72 h using different concentrations (1 µM, 2.5 µM, 5 µM, 10 µM, 25 µM, 50 µM, and 100 µM) of standard Doxorubicin and extract dissolved in DMSO. 50 µL of the XTT labelling mixture was mixed with 100 µL of growth medium in the individual well of the 96-well culture plate. A set of blanks was also included for each condition. Absorbance for both untreated and treated cultures was recorded 4 h after XTT addition. Net absorbances (A450–A620) were calculated. Per condition, the mean net absorbance of all replicates was calculated by subtracting the mean of the blanks, and the mean cell proliferation after 72 h of treatment was expressed as a percentage of cell survival. Phase-contrast and fluorescence microscopy images were captured using NIKON at a 20X objective on an Inverted fluorescence microscopy system. 4′,6-diamidino-2-phenylindole containing mounting medium was used to mount, and Fluorescein diacetate was used to stain the cells. Beta-actin primary antibody (1:500) was used after cell fixation with 4% paraformaldehyde. The IC_{50} values were calculated[23-25].

2.9 *In Vivo* Studies

2.9.1 Procurement and Maintenance of Experimental Animals

Adult Wistar rats of both sexes (8-12 weeks old, weighing 150-180 g) were procured from Mahaveera Enterprises, Hyderabad. All the rats were kept according to the standard laboratory conditions (20 ± 2°C, 45-55% relative humidity). The rats were allowed to access rat feed and water under stringent hygienic conditions. The study was conducted as per the guidelines of the Committee for Control and Supervision of Experiments on Animals, CCSEA (DSOP/IAEC/DEC-2021/01). The study design is divided into five groups, each group with six rats in it.

Group I: Control - aqueous 1% carboxymethyl cellulose, 10 ml/kg b.w

Group II: Hepatotoxic – Isoniazid + rifampicin, 50 mg/kg +100 mg/kg b.w

Group III: Standard – (Isoniazid + rifampicin) + silymarin 100 mg/kg b.w

Group IV: Low dose - (Isoniazid + rifampicin) + *P. acidus* bark extract**,** 200 mg/kg b.w

Group V: High dose - (Isoniazid + rifampicin) + *P. acidus* bark extract**,** 400 mg/kg b.w

Rats were observed all the days for their behavioural and stool consistency during the treatment period. After 28 days of treatment, rats were sacrificed under anaesthesia (anaesthetic ether) by cervical dislocation, and the blood and liver were taken for assessment of different parameters[26-28].

2.9.2 Body and Liver Weights

The rats were weighed upon completion of the treatment period and sacrificed. The isolated livers were placed on an icy cold plate, fat and mesentery were removed, and then placed on filter paper for weighing, and the weight was expressed in grams[29].

2.9.3 Blood-serum Parameters

3mL vacuum tubes were used for blood sample collection, and the collected samples were centrifuged at 3000 rpm (10 mins). 100 µL supernatant layer was made ready based on the Erba (India) kits. All biomarker levels, Serum glutamate oxaloacetate transaminase level (AST), serum glutamate pyruvate transaminase level (ALT), Alkaline Phosphatase level (ALP), Total Bilirubin (TBI) and Direct Bilirubin (DBI) were estimated by autoanalyser[25].

2.9.4 Oxidative stress parameters

The liver homogenates were prepared in phosphate buffer. First, centrifugation was performed for 5 min at 800 rpm. The supernatant layer was used for the analysis of myeloperoxidase (MPO), Malondialdehyde (MDA), and Glutathione (GSH). The remaining homogenates were centrifuged at 10,500 rpm (15min). The post-mitochondrial supernatant obtained was analysed for catalase (CAT) and Superoxide Dismutase (SOD) using Sigma-Aldrich kits by spectrophotometer[29-33].

2.9.5 Inflammatory Cytokine Parameters

Inflammatory cytokines, tumour necrosis factor-α (TNF-α), interleukin-6 (IL-6), interleukin - 8 (IL-8), and interleukin-1β (IL-1β) were estimated in the serum samples using a simple ELISA kit, and the

above-mentioned cytokine contents in the samples were determined from the standard curve[34].

2.9.6 Histopathology of Liver

Fragments of liver were fixed in 10% solution of neutral formalin, embedded in paraffin, and 6 mm-sized sections were stained with hematoxylin-eosin (HandE), toluidine blue (TB), and Goldner's masson trichrome (MT) stain and observed under a light microscope for any pathological alterations, and photomicrographs were recorded[27,35,36].

2.10 Statistical Analysis

Data collected were indicated as means and standard deviations (Mean±SD) and processed using GraphPad Prism software (version 10.0). $p<0.05$ is considered statistically significant.

3. Results and Discussion

3.1 Quantitative Estimations

The *P. acidus* bark has reported 39.00±1.00% g/g of terpenoid content. Terpenoids are a sundry class of naturally existing organic components acquired from the isoprene (C_5) unit. They play important roles in many biological activities and have a broad range of pharmacological actions. They have displayed actions like antiviral, antimicrobial, antiulcer, antihelminthic, anti-inflammatory, antioxidant, larvicidal and insecticidal. Their diversity and versatility have made them worthwhile compounds with potential utilisations in different domains, from medicinal to pest management and many more[37]. The standard graph of gallic acid ($y = 0.0251x + 0.0941$, $R^2 = 0.9894$) estimated 28.13±0.005 mg GAE/g phenolic content and 351.70±0.993 mg QE/g flavonoid content from the quercetin standard curve ($y = 0.0012x + 0.1493$, $R^2 = 0.961$) in bark extract. Thus, it indicates that *P. acidus* bark extract may have good antioxidant properties. Flavonoids and many other phenolic compounds are popularly well-known secondary metabolites which carry an aromatic ring with at least one hydroxyl group. These phytoconstituents are available in herbal medicines and nutrients; both flavonoids and other phenolic compounds have been demonstrated as potential antioxidants, anti-inflammatory, anticancer, cardioprotective agents, skin protection from UV radiation, antibacterial, immune system promoting, and also interesting candidates for medical and pharmaceutical applications[38].

3.2 *In Vitro* Determination of Antioxidant Activity

Drug-induced hepatic damage can cause a sharp fall in liver activities and acute liver failure. Drugs causing hepatotoxicity may lead to the concentration of reactive oxygen species or reactive nitrogen species and cause oxidative or nitrosative stress in the liver by various mechanisms, including the elevation in intracellular oxidisers, depletion of antioxidants, lipid peroxidation, and mitochondrial malfunction[39]. The free radical scavenging activities of *P. acidus* bark are estimated by DPPH, reducing power and nitric oxide assays. Reacting with DPPH, antioxidants transfer an electron/hydrogen to DPPH, thus counterpoise its free radical ability. Therefore, at 518 nm, its absorption corresponds to the quantity of DPPH remaining[40]. The result in the graph (Figure 1 (A)) displays the significant scavenging capacity of bark, showing an IC_{50} value of 216.41 ± 0.189 µg/mL and a standard produced scavenging activity of 95.48 ± 0.760 µg/mL. The reducing power procedure is grounded in the basis that the substances, which have reducing ability, interact with potassium ferricyanide (Fe^{3+}) to get converted to potassium ferrocyanide (Fe^{2+}), which further interacts with ferric chloride to produce a ferric–ferrous complex, which has a maximum absorption at 700 nm[41]. The reducing potential indicates a good linear relation in both the extract and the standard (Figure 1 (B)). The IC_{50} values of the bark and the standard are estimated as 191.65±0.142 µg/mL and 89.59±0.090 µg/mL, respectively. Nitric oxide was produced from the spontaneous breakdown of sodium nitroprusside in phosphate buffer, which further reacts with oxygen molecules to develop nitrite ions, and additionally, it is checked by the Griess reactions[42]. The bark extract exerts its potential in a dose-dependent fashion (Figure 1 (C)). 85.25±0.107 µg/mL and 188±0.140 µg/mL are calculated as IC_{50} values for the standard and extract, respectively. The results of the assay showed that the extract has weak nitric oxide scavenging potential in comparison with the standard ascorbic acid.

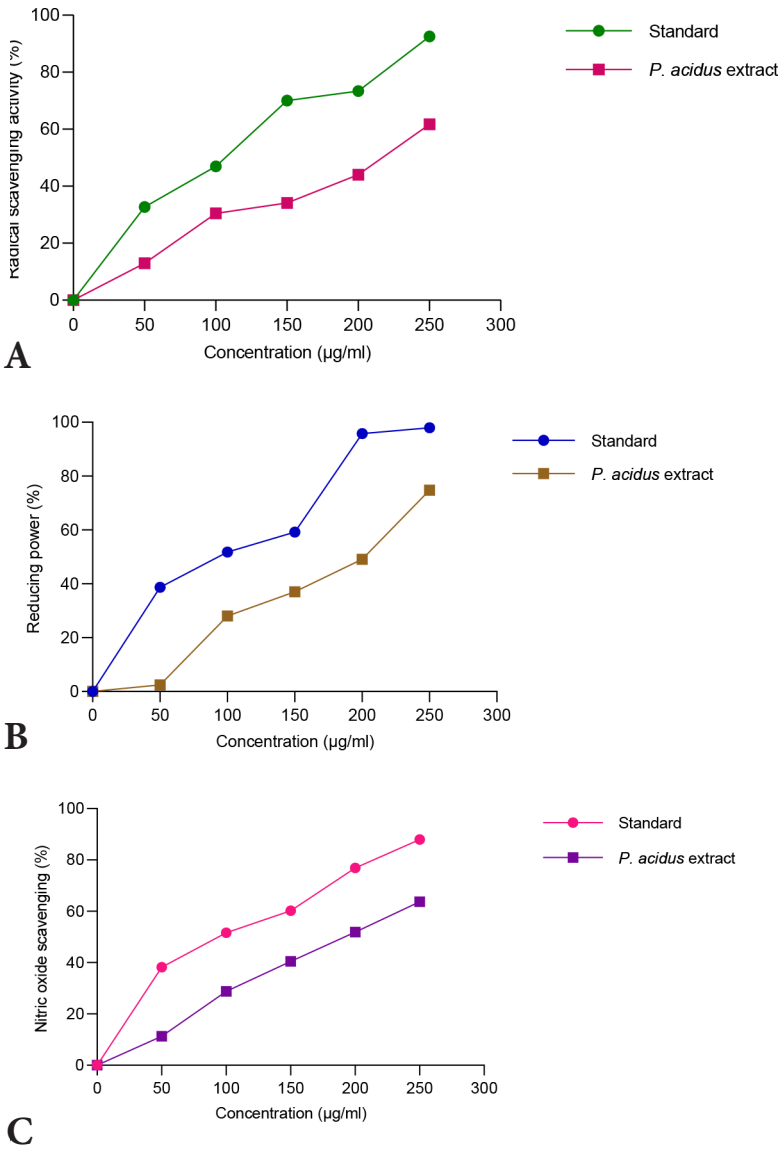


Figure 1. Graphs of antioxidant activities of *P. acidus* bark showing **(A).** DPPH assay, **(B).** Reducing power assay and **(C).** Nitric oxide assay.

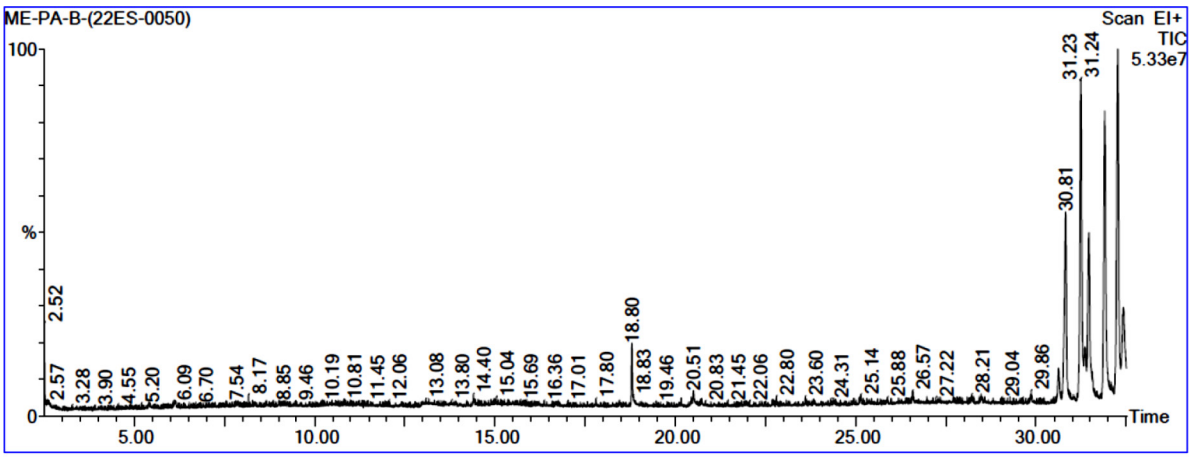
3.3 Gas Chromatography-Mass Spectrometry Analysis

Medicinal plants are the reservoirs of novel medicines. Numerous modern medicines have been developed indirectly from them. They have provided diverse components to combat different medical conditions and illnesses. The extraction and analysis of herbal materials have a valuable function in the improvement, revampment and quality control of herb-based formulations[43]. The GCMS analysis of *P. acidus* bark was utilised to find out the bioactive components present in it. The mass spectra of the bioactive principles in the bark extract, with their molecular formula, molecular weight, Retention Time (RT), and area% (concentration), are shown in Figure 2 and Table 1. It shows the nine bioactive principles in the extract. Among the identified bioactive principles (C9) Kauran-18-al, 17-(acetyloxy)-, (4.beta.)- and (C8) Cis-Z-. Alpha-bisabolene epoxide is present at a maximum of 24.8% and 22.8%, respectively.

3.4 Molecular Docking

The molecular docking method has emerged as a popular facet of *in silico* drug design in modern times. This method entails predicting the interaction between a molecule and a protein at the atomic scale. It focuses

on the prediction of the ligand-receptor complex by computer-based techniques. The methodology of docking involves two main steps: firstly, sampling the ligand and secondly, utilising a scoring function[44]. PDB ID: 5HYK was selected for the docking studies. All the docking scores and dG binding values of the phytoconstituents reported in the GCMS investigation of the extract are displayed in Table 2, and their 2D



#	RT	Scan	Height	Area	Area %	Norm %
1	2.518	4	13,379,505	155,607.2	1.336	5.39
2	18.800	3259	8,997,294	289,969.0	2.490	10.05
3	30.620	5622	4,471,131	214,909.8	1.846	7.45
4	30.815	5661	26,866,090	1,721,981.2	14.789	59.69
5	31.240	5746	43,745,484	2,413,970.8	20.732	83.67
6	31.355	5769	3,033,348	128,144.9	1.101	4.44
7	31.460	5790	20,627,712	1,178,849.1	10.124	40.86
8	31.895	5877	41,063,428	2,655,324.8	22.805	92.04
9	32.260	5950	48,007,344	2,885,071.0	24.778	100.00

Figure 2. The resultant spectra of *P. acidus* bark using GC-MS analysis.

Table 1. Results of GC-MS investigation of the extract of *P. acidus* bark

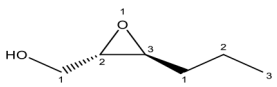
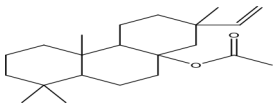
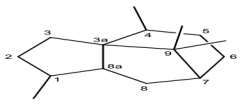
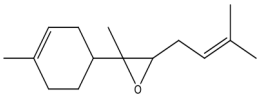
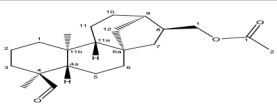
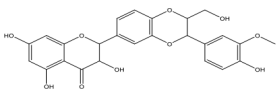
Compound No.	Peak name	Molecular formula	Molecular weight	Retention time
C1	Cyclopropyl carbinol	C_4H_8O	72	2.518
C2	(2S,3S)-(-)-3-Propyl Oxiranemethanol	$C_6H_{12}O_2$	116	18.8
C3	2-Amino Nonadecane	$C_{19}H_{41}N$	283	30.62
C4	8A(2H)-Phenanthrenol, 7-Ethenyldodecahydro-1,1,4A,7-Tetramethyl-, A	$C_{22}H_{36}O_2$	332	30.815
C5	Diazo progesterone	$C_{21}H_{30}N_4$	338	31.24
C6	1H-3A,7-Methanoazulene, Octahydro-1,4,9,9-tetramethyl-	$C_{15}H_{26}$	206	31.355
C7	1H-3A,7-Methanoazulene, octahydro-1,4,9,9-tetramethyl-	$C_{15}H_{26}$	206	31.46
C8	Cis-Z-.Alpha.-bisabolene epoxide	$C_{15}H_{24}O$	220	31.895
C9	Kauran-18-al, 17-(acetyloxy)-, (4.beta.)-	$C_{22}H_{34}O_3$	346	32.26

and 3D images of the interactions with the receptor are shown in Figure 3. Among the nine bioactive constituents, one compound has not been reported with a dG binding; therefore, eight bioactive compounds and a reference standard, silymarin, are studied here. The lowest docking score value of silymarin refers to the high affinity for the receptor. Among the nine bioactive constituents, Kauran-18-al, 17-(acetyloxy)-, (4.beta.)- has the closest docking score to Silymarin. Table 3 depicts the hydrogen-bonding interactions and the bond-length distances of the bioactive compounds and the receptor. Furthermore, the ADME and toxicity predictions of the bioactive constituents were also studied (Tables 4 and 5). It predicts the bioavailability, distribution in the body, metabolism, excretion pathways, and also assess the toxicological risk associated with them.

3.5 XTT Cell Proliferation Assay

This method uses 2,3-bis-(2-methoxy-4-nitro-5-sulfophenyl)-2H-tetrazolium-5-carboxanilide (XTT), a second-generation water-soluble variant of the tetrazolium salt 3-(4,5-Dimethylthiazol-2-yl)-2,5-diphenyltetrazolium bromide (MTT). It estimates proliferation grounded in the metabolic activities of the cells and is routinely utilised in 2D culture states[45]. XTT is a colourless tetrazolium salt, which transforms to a coloured formazan (water-soluble derivative) by the enzyme succinate dehydrogenase, as it is involved in the energy supply of each living cell[46]. In this study, HepG2 cell lines were used, and Doxorubicin was the standard drug. A dose-dependent effect of the extract was noticed (Figure 4); the lowest percentage of cell survival for the extract was observed at 100µM on HepG2 cells (26.16±3.85) compared to the control

Table 2. Dock score and dG binding values of phytoconstituents of extract *P. acidus* bark reported in GCMS analysis

S. No.	Compound name	2D structure	Dock score	dG binding
1	Cyclopropyl carbinol		-4.044	-30.75
2	(2S,3S)-(-)-3-Propyl Oxiranemethanol		-5.487	-49.94
3	2-Amino Nonadecane		-4.584	-94.01
4	8A(2H)-Phenanthrenol, 7-Ethenyldodecahydro-1,1,4A,7-Tetramethyl-, A		-4.489	-29.51
5	1H-3A,7-Methanoazulene, Octahydro-1,4,9,9-tetramethyl-		-7.951	-48.44
6	1H-3A,7-Methanoazulene, octahydro-1,4,9,9-tetramethyl-		-7.951	-48.44
7	Cis-Z-.Alpha.-bisabolene epoxide		-8.008	-91.10
8	Kauran-18-al, 17-(acetyloxy)-, (4.beta.)-		-9.583	-55.89
9	Standard Silymarin		-13.608	-79.52

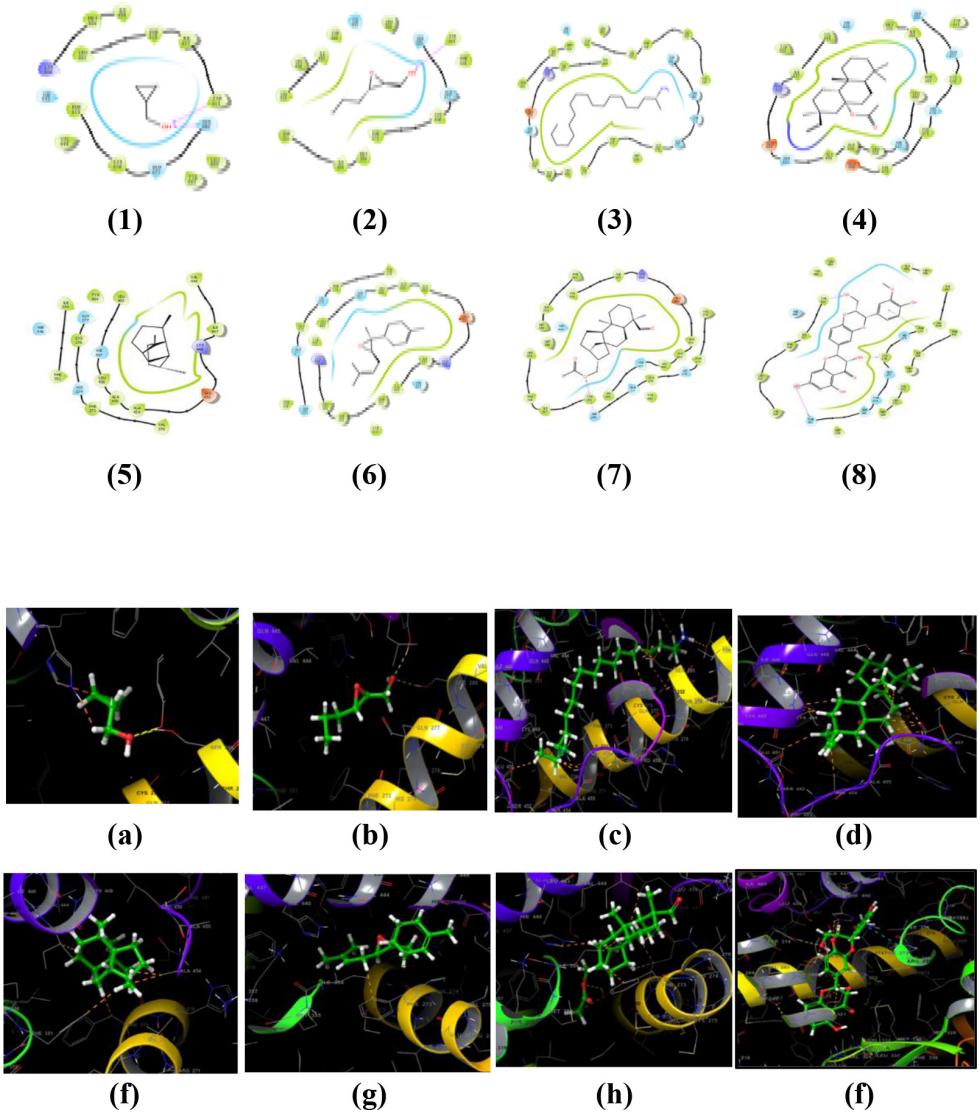


Figure 3. 2D and 3D images of the binding interactions of all phytoconstituents of *P. acidus* bark with the receptor reported in GCMS analysis.

Table 3. Hydrogen-bonding 2D interactions and bond length distance of phytoconstituents of *P. acidus* bark

S. No.	Compound name	2D Interaction	Distance (Å)
1	Cyclopropyl carbinol	H-bond: TYR314, SER280	1.88,2.25
2	(2S,3S)-(-)-3-Propyl oxiranemethanol	H-bond: TYR314	2.14
3	2-Amino Nonadecane	No interaction	No distance
4	8A(2H)-Phenanthrenol, 7ethenyldodecahydro-1,1,4A,7-tetramethyl-, A	No interaction	No distance
5	1H-3A,7-methanoazulene, octahydro-1,4,9,9-tetramethyl-	No interaction	No distance
6	1H-3A,7-Methanoazulene, octahydro-1,4,9,9-tetramethyl-	No interaction	No distance
7	Cis-Z-.Alpha.-bisabolene epoxide	No interaction	No distance
8	Kauran-18-al, 17-(acetyloxy)-, (4.beta.)-	H-bond: SER280	2.17
9	Standard Silymarin	H-bond: CYS276, TYR314, THR283 Pi-Pi Stacking: PHE273	2.44,2.20,1.88 5.02

Table 4. ADME prediction of phytoconstituents of *P. acidus* bark

S. No.	Compound name	MW g/mol	H-bond Acceptor	H-bond Donors	Log P	GI Absorption	BBB permeation	Bioavailability score	Lipinskin Violation	Synthetic Accessibility
1	Cyclopropyl carbinol	72.1	1	1	1.42	High	No	0.55	0	1.00
2	(2S,3S)-(-)-3-Propyl Oxiranemethanol	116.2	2	1	1.92	High	Yes	0.55	0	2.61
3	2-Amino Nonadecane	283.5	1	1	5.13	Low	No	0.55	1	2.87
4	8A(2H)-Phenanthrenol, 7-Ethenyldode cahydro-1,1,4A,7-Tetramethyl-, A	332.5	2	0	3.95	High	No	0.55	1	4.27
5	1H-3A,7-Methanoazulene, Octahydro-1,4,9,9-tetramethyl-	206.4	0	0	3.22	Low	No	0.55	1	4.60
6	1H-3A,7-Methanoazulene, octahydro-1,4,9,9-tetramethyl-	206.4	0	0	3.22	Low	No	0.55	1	4.60
7	Cis-Z-.Alpha.-bisabolene epoxide	220.4	1	0	3.63	High	Yes	0.55	0	4.23
8	Kauran-18-al, 17-(acetyloxy)-, (4.beta.)-	346.5	3	0	3.48	High	Yes	0.55	1	5.25
9	Standard Silymarin	482.4	10	5	2.79	Low	No	0.55	0	4.92

(untreated cells) and was relatively lower when compared to the same concentration of the standard drug (34.38±6.95). The IC_{50} values of the *P. acidus* bark extract and Doxorubicin were 57.59 µM and 5.99 µM, respectively. Phase-contrast and fluorescence microscopy images of *P. acidus* extract cytotoxicity are displayed in Figures 5 and 6, respectively.

3.6 *In Vivo* Studies

3.6.1 Body and Liver Weights

The body weights of the rats before and after the treatments were measured, and their weight differences were calculated (Table 6) after completion of the administration period. The Group I rats showed an increase in weight, and the weight difference was observed to be 11.67±1.63 g. Group II (INH and RFP) demonstrated a decrease in body weight with a weight difference of 3.00±1.41 g. The extract of *P. acidus* group IV and group V (200 mg/kg and 400 mg/kg, respectively) displayed a decline in body weight when compared with group I (Control).

INH- and RFP administered rats had significantly increased liver weight to 9.71±0.20 g when compared to the control (8.23±0.72g). Among the treatments of 200 and 400 mg/kg *P. acidus* extract, the 400 mg/kg treated group significantly reduced liver weight to 8.32±0.43 g, compared to INH and RFP treatment. The standard-treated Group III remarkably reduced liver weight (Table 6).

3.6.2 Blood-serum Parameters

The rats were distressed with hepatotoxic drugs (INH and RFP), which led to hepatic cell damage and augmentation, centrilobular necrosis, steatosis, and hampering of the endogenous antioxidant system. Furthermore, leads to the rise of serum enzymes (ALT,

Table 5. Toxicity prediction of phytoconstituents of *P. acidus* bark

S. No.	Compound name	AMES toxicity (yes/ no)	Max. tolerated dose in humans (log g/kg/ day)	hERG I inhibitor (yes/no)	hERG II inhibitor (yes/no)	Oral rat acute toxicity (LD_{50}) (mol/ kg)	Oral rat chronic toxicity (LOAEL) (log mg/ kg_bw/ day)	Hepato-toxicity (yes/ no)	Skin sensiti sation (yes/ no)	*T. pyriformis* toxicity (log µg/L)	Minnow toxicity (log mM)
1	Cyclopropyl carbinol	No	1.116	No	No	1.835	1.58	No	No	-1.558	2.394
2	(2S,3S)-(-)-3-Propyl Oxiranemethanol	Yes	0.936	No	No	2.036	2.418	No	Yes	-1.222	2.414
3	2-Amino Nonadecane	No	-0.943	No	Yes	2.392	1.716	No	Yes	1.43	-0.58
4	8A(2H)-Phenanthrenol, 7-Ethenyldode cahydro-1,1,4A,7-Tetramethyl-, A	No	-0.111	No	No	1.775	1.941	No	No	1.537	-0.207
5	1H-3A,7-Methanoazulene, Octahydro-1,4,9,9-tetramethyl-	Yes	-0.111	No	No	1.695	1.402	No	No	1.437	-0.081
6	1H-3A,7-Methanoazulene, octahydro-1,4,9,9-tetramethyl-	No	-0.111	No	No	1.695	1.402	No	No	1.437	-0.081
7	Cis-Z-.Alpha.-bisabolene epoxide	No	0.226	No	No	1.474	1.178	No	Yes	1.449	0.565
8	Kauran-18-al, 17-(acetyloxy)-, (4.beta.)-	No	-0.24	No	No	2.076	1.985	No	No	0.535	-0.649
9	Standard Silymarin	Yes	0.866	No	Yes	2.631	3.473	No	No	0.285	2.994

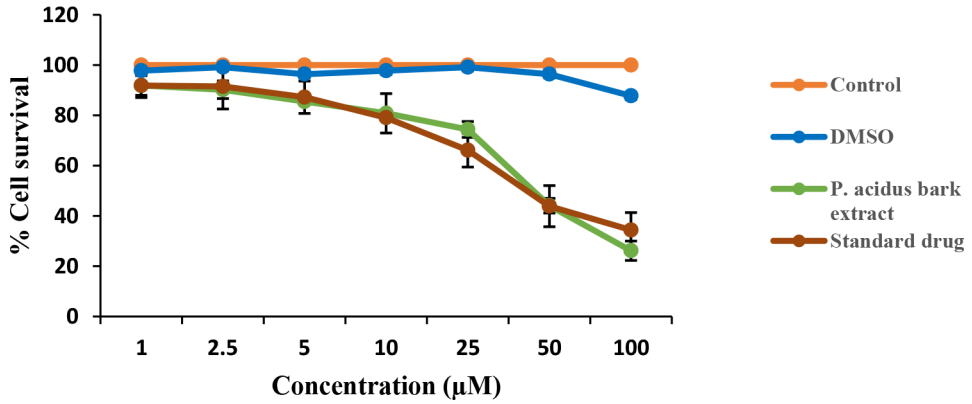


Figure 4. Cytotoxic effects of *P. acidus* bark against the HepG2 cell line. The standard drug, Doxorubicin, served as a positive control.

AST, ALP, and TBI) due to their leakage from the liver. These liver enzymes are helpful quantitative indicators and also reflect the nature of hepatic cellular injury[47]. The hepatotoxic drugs INH and RFP have produced a phenomenal rise in the liver enzymes in serum. In both dose levels of *P. acidus*, 400 mg/kg displayed the most significant protection of liver injury from INH and RFP, thereby maintaining the serum enzyme levels ALT, AST, ALP, DBI, and TBI (Figure 7), which were almost comparable to the control and standard silymarin. There was no effective protection was observed with the 200 mg/kg extract dose.

3.6.3 Oxidative Stress Parameters

Oxidative stress and elevated levels of free radicals are associated with hepatopathy, as a consequence of reduced scavenging potential of the hepatocytes[48]. The human body has a powerful defence system to protect and nullify the free radical-caused injury. This is accomplished by a set of endogenous antioxidant enzymes such as superoxide dismutase and catalase. Suppression of the body's antioxidant mechanism in anti-tubercular drug-induced rats has been revealed earlier[49]. The suppression of the antioxidant system and/or increase in free radical output leads to imbalance

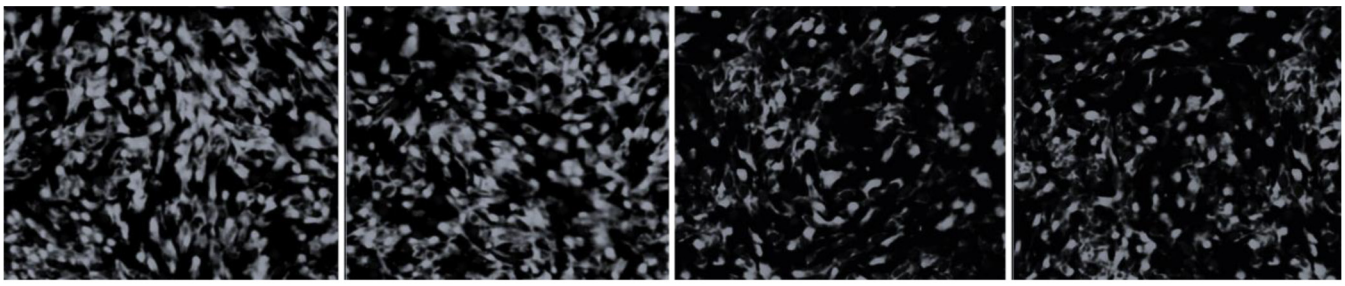


Figure 5. Phase-contrast microscopy images showing cytotoxic effects of *P. acidus* bark against the HepG2 cell line.

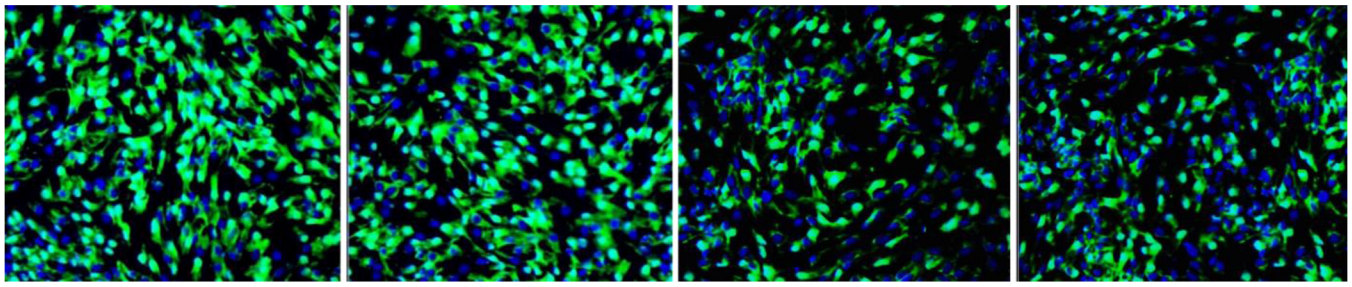


Figure 6. Fluorescence microscopy images of HepG2 cells after 72 h of treatment with the IC_{50} concentration of the extract of *P. acidus* bark.

Table 6. Weights of body and rat liver treated with *P. acidus* extract before and after treatments

	Control	Isoniazid + Rifampicin	Silymarin	*P. acidus* extract, 200 mg/kg	*P. acidus* extract, 400 mg/kg
0^{th} Day weights (Grams)	181.17±0.60	184.17±0.75	186.50±0.43	188.83±0.65	190.50±0.43
28^{th} Day weights (Grams)	192.83±1.08	181.17±0.95	179.00±0.37	185.67±0.80	185.00±0.45
Weight difference (Grams)	$11.67\pm1.6^{3\#\#\#\#}\#$	3.00±1.41	7.50±0.55****	3.17±1.17**	5.50±0.55***
Liver weights (Grams)	$8.23\pm0.72^{\#\#\#\#}$	9.71±0.20	7.75±0.44****	8.73 ± 0.50^{ns}	8.32±0.43**

The data were examined by one-way ANOVA and expressed as mean ± SD (n = 6). Post hoc Dunnett's method was used to compare groups vs. INH and RFP. pvalues: $^{\#\#\#\#}$<0.0001 vs control Group I. pvalues: ^{ns}p>0.05,**p<0.01, ***p<0.001 and ****p<0.0001 vs Group II (against INH and RFP)

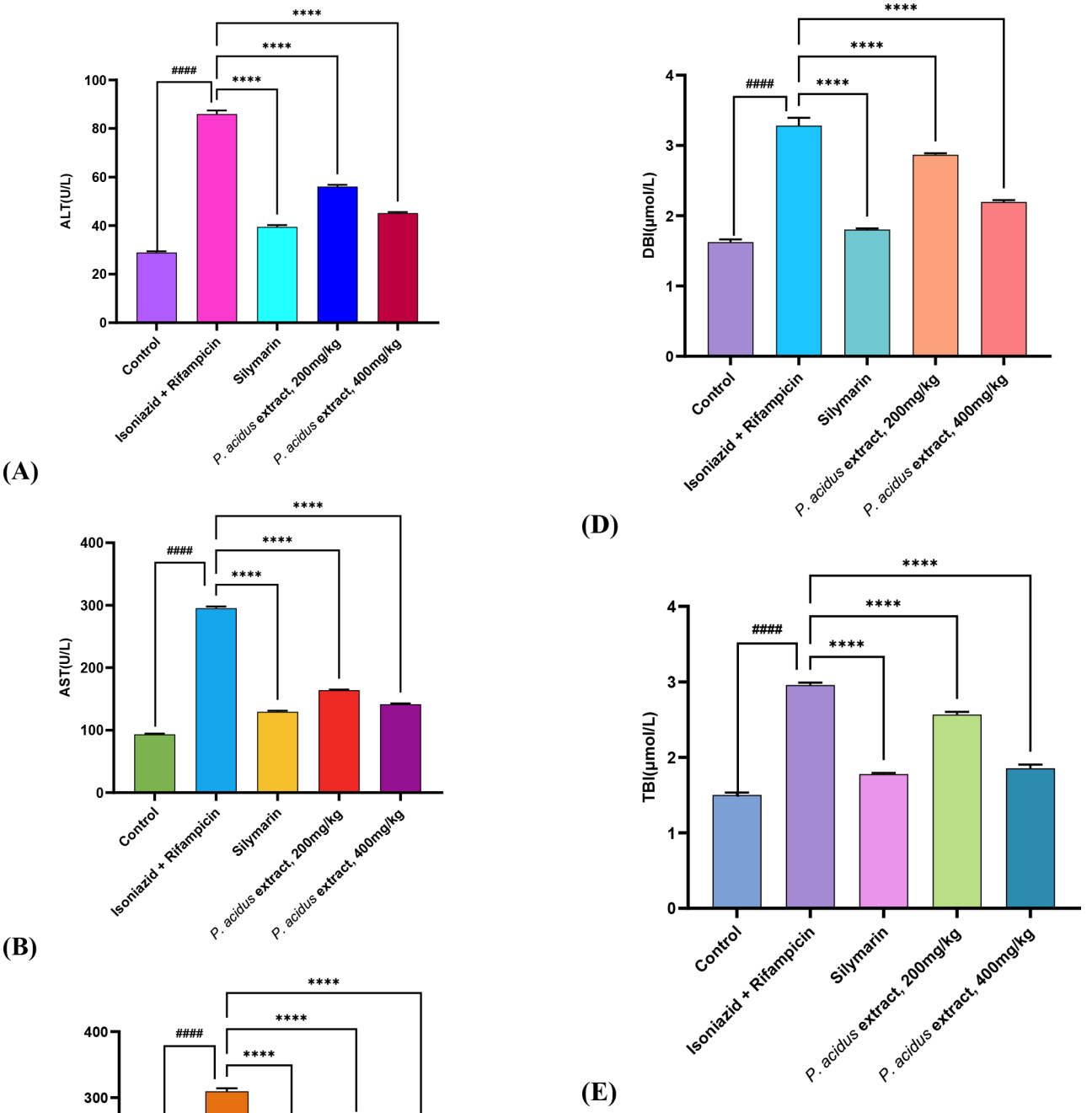
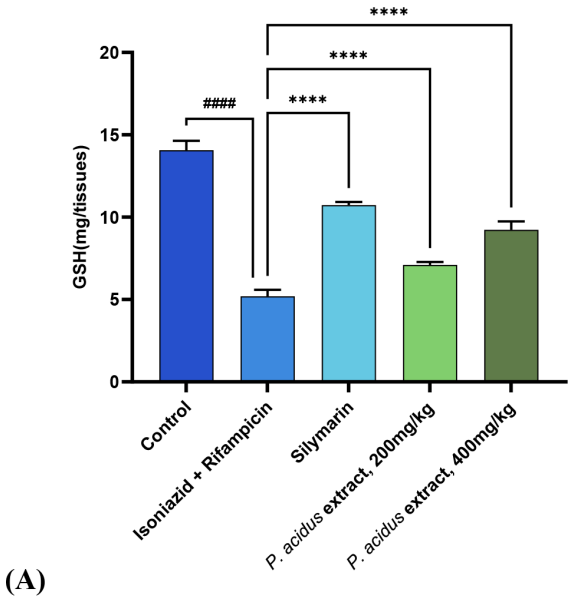
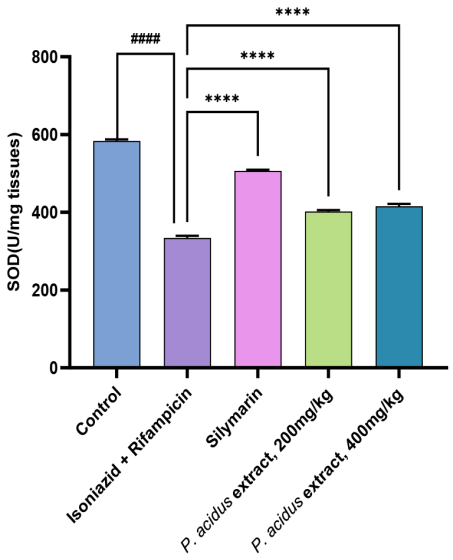


Figure 7. Effect of *P. acidus* bark extract on blood serum parameters: **(A).** ALT, **(B).** AST, **(C).** ALP, **(D).** DBI and **(E).** TBI against INH and RFP-induced hepatotoxicity in rats. The data were examined by one-way ANOVA and expressed as mean ± SD (n = 6). Post hoc Dunnett's method was used to compare groups vs INH and RFP. pvalues: ####<0.0001 vs control Group I. pvalues: ****<0.0001 vs Group II (against INH and RFP).

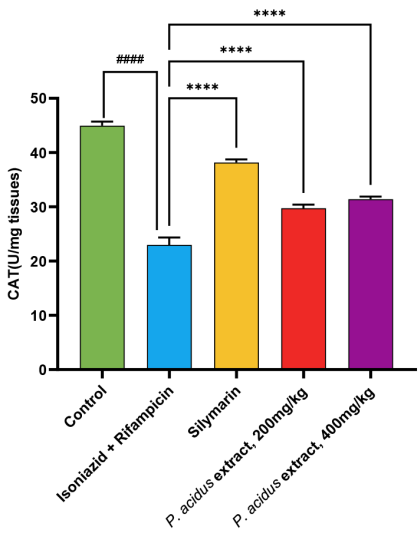
of the prooxidant-antioxidant equilibrium, causing oxidative stress-induced cellular death[50]. Decrease of reduced glutathione is the result of increased lipid



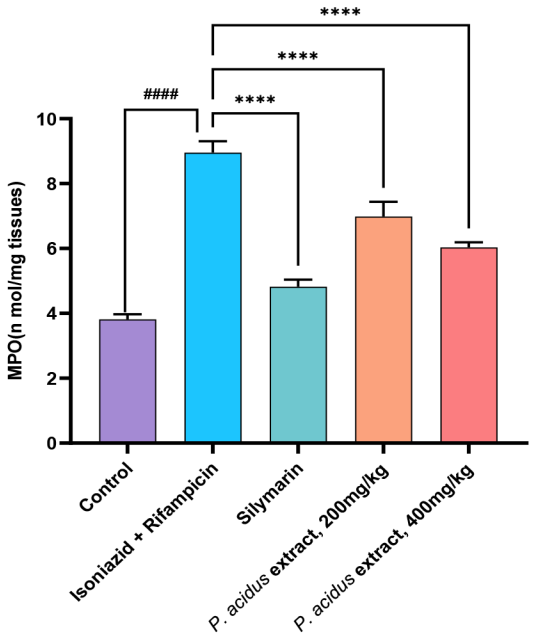
(A)



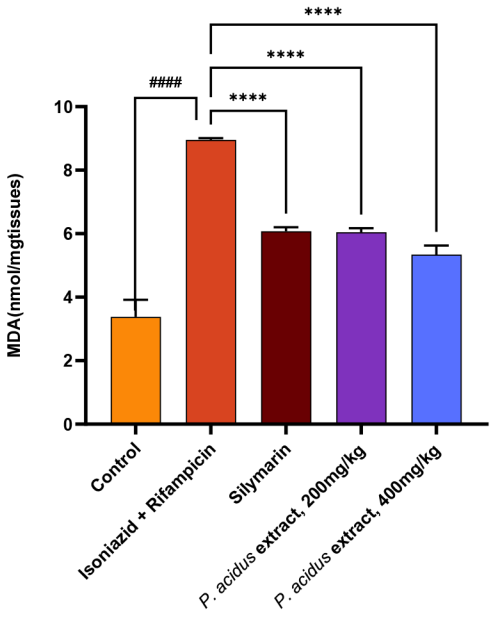
(B)



(C)



(D)



(E)

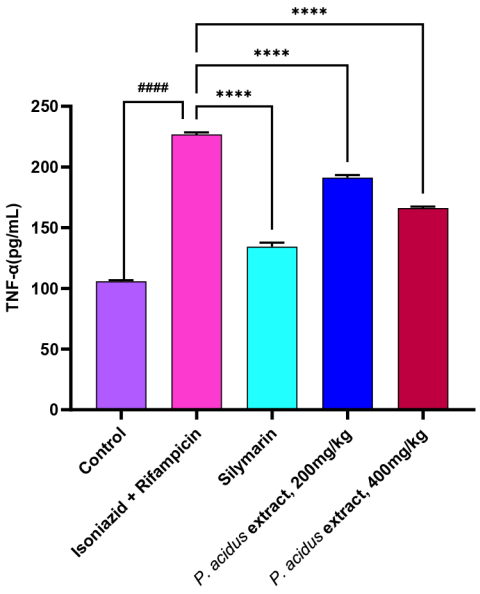
Figure 8. Effect of *P. acidus* bark extract on oxidative stress parameters: **(A).** GSH, **(B).** SOD, **(C).** CAT, **(D).** MPO, and **(E).** MDA against INH and RFP-induced hepatotoxicity in rats. The data were examined by one-way ANOVA and expressed as mean ± SD (n = 6). Post hoc Dunnett's method was used to compare groups vs INH and RFP. pvalues: ####<0.0001 vs control Group I. pvalues: ****<0.0001 vs Group II (against INH and RFP).

peroxidation, which causes more glutathione uptake[51]. The GSH, SOD and CAT amounts had notably declined in the *P. acidus* extract doses group, whereas the INH

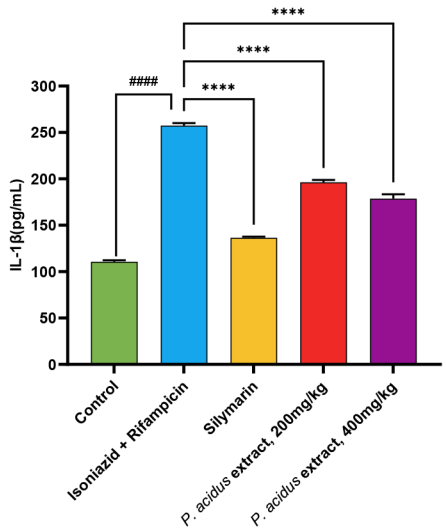
and RFP group had shown a remarkable decrease in these levels in comparison with the control. Figure 8 indicates a noteworthy change in the oxidative stress parameter levels in INH and RFP induced rats, as p<0.0001in comparison to the control group. Administration of bark extract at the doses of 200 and 400 mg/kg considerably prevented the rise in MDA and MPO levels. Enhanced MPO activity is an indicator of neutrophil infiltration which shows the inflammatory damaging activity in liver tissues. It has been associated with another enzymatic pathway in the onset of INH and RFP hepatic toxicity[52]. These levels were close to normal in the silymarin-served group when compared to the INH and RFP group.

3.6.4 *Inflammatory Cytokine Parameters*

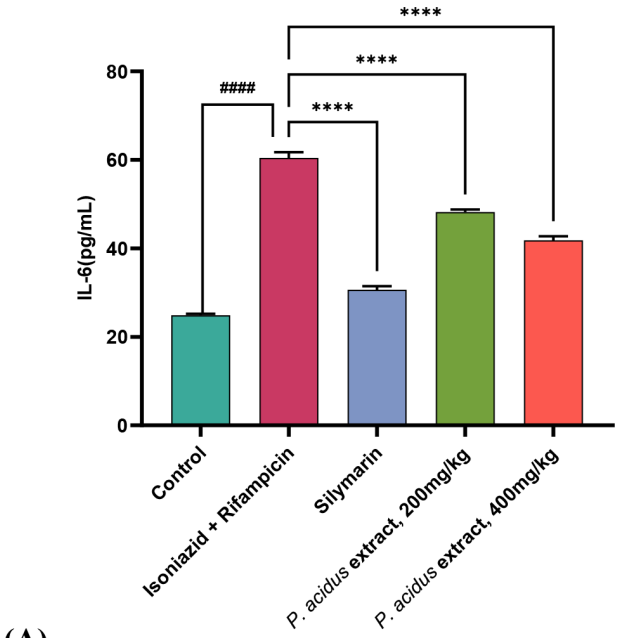
Besides oxidative stress, apoptotic pathways and inflammatory cytokines also play important roles in



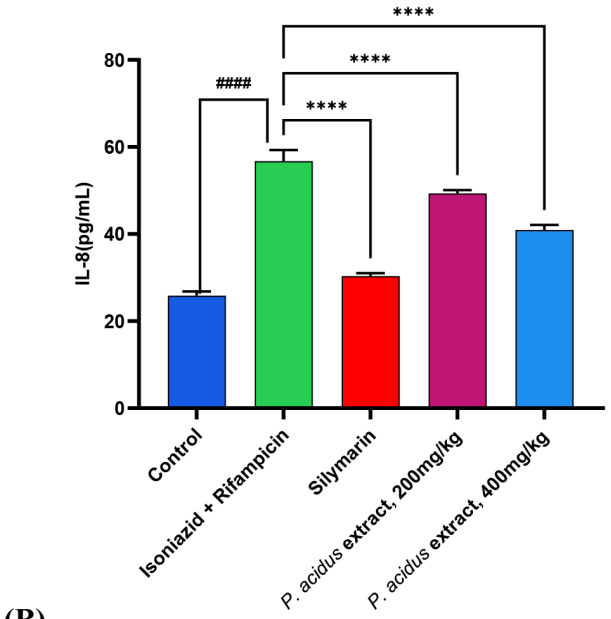
(C)



(D)

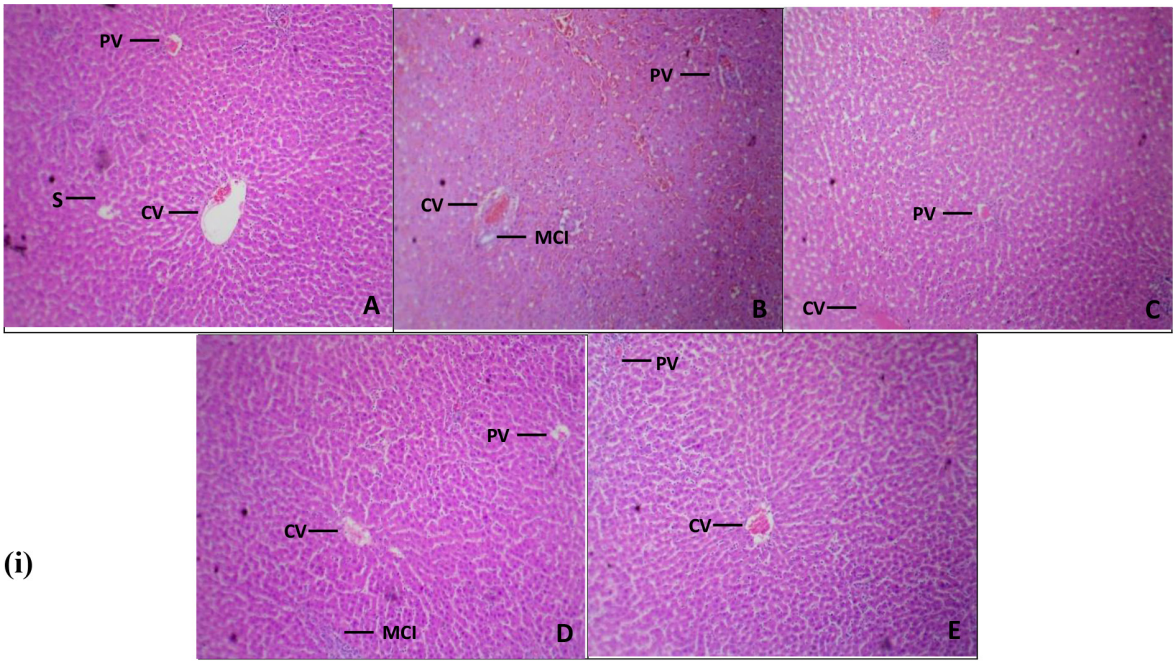


(A)

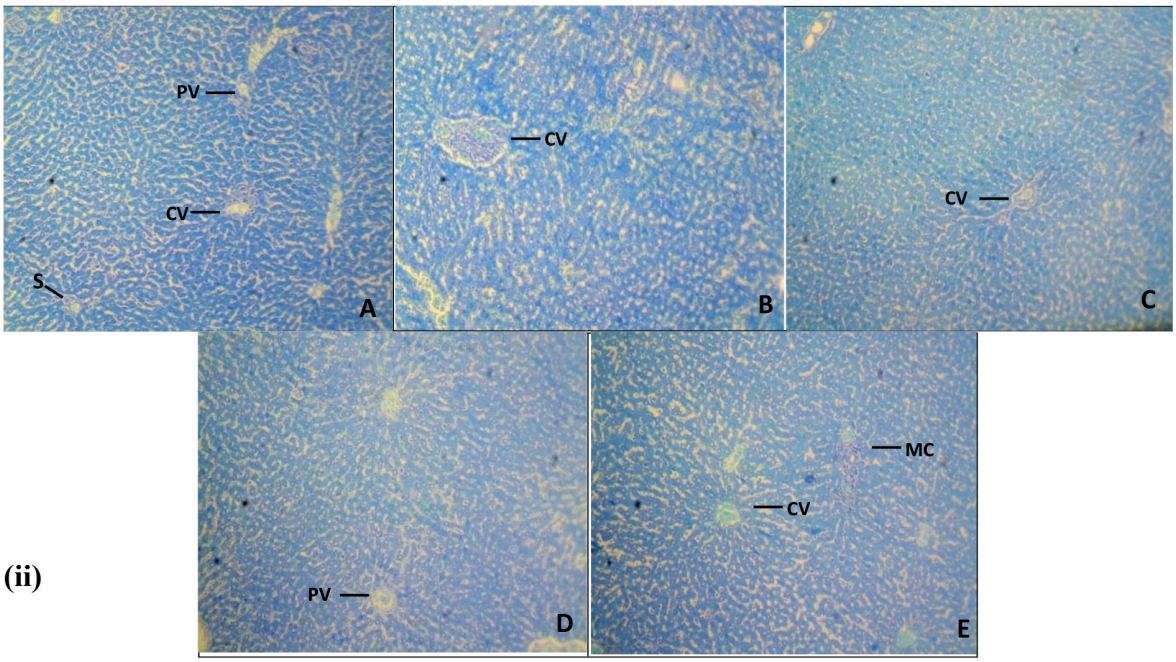


(B)

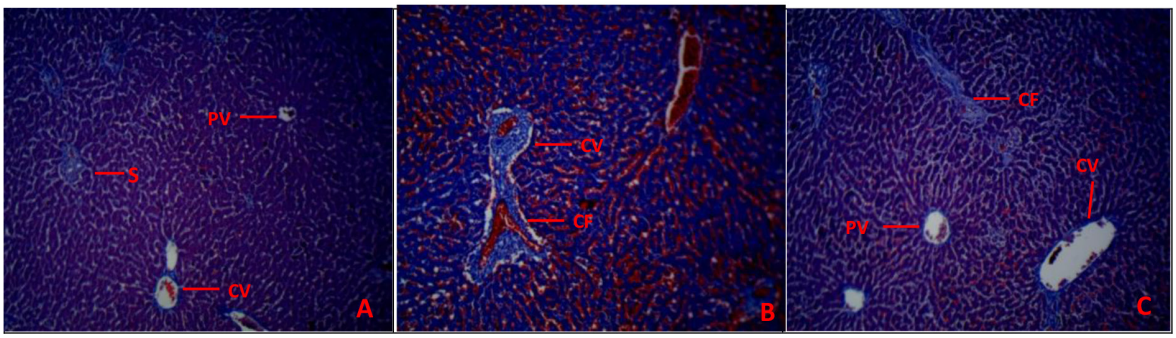
Figure 9. Effect of *P. acidus* bark extract on inflammatory cytokines **(A).** IL-6, **(B).** IL-8, **(C).** TNF-α, and **(D).** IL-1β against INH and RFP-induced hepatotoxicity in rats. The data were examined by one-way ANOVA and expressed as mean ± SD (n = 6). Post hoc Dunnett's method was used to compare groups vs. INH and RFP. pvalues: ####<0.0001 vs control Group I. pvalues: ****<0.0001 vs Group II (against INH and RFP).


PV
S
CV
A
PV
CV
MCI
B
PV
CV
C
PV
CV
MCI
D
PV
CV
E

(i)


PV
CV
S
A
CV
B
CV
C
PV
D
MC
CV
E

(ii)


PV
S
CV
A
CV
CF
B
CF
CV
PV
C

(iii)

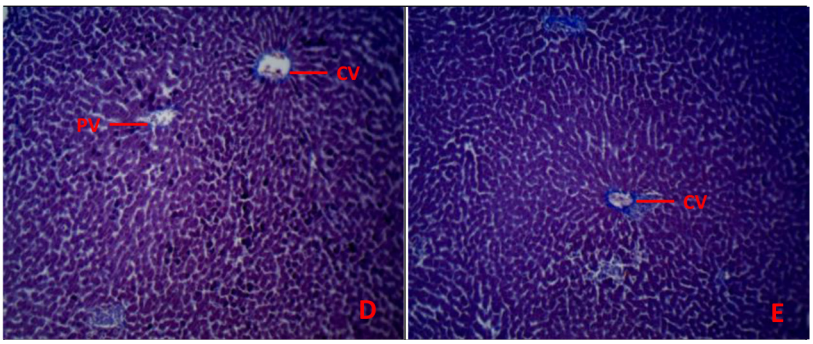


Figure 10. The histopathological images of three different stains: **(i)** Hematoxylin and eosin (HandE) stain, **(ii)** Toluidine blue stain and **(iii)** Masson's trichrome stain. Each stain represents different groups of treatments. **(A)** control group, **(B)** INH and RFP, **(C)** bark extract 200 mg/kg, **(D)** bark extract 400 mg/kg, and **(E)** Silymarin. Magnification 10X. *Histological abbreviations:* PV = Portal Vein, CV = Central Vein, S = Sinusoid, MCI = Mononuclear Cellular Infiltration, MC = Mast Cells, CF = Collagen Fibre.

anti-TB drug-related hepatic damage. Cytokines, a kind of protein, are associated with immunological reactions, inflammation, tissue damage, and organ malfunction. Apoptosis occurs through an enzymatic mechanism and requires caspase 3 and caspase 9. These enzymes are responsible for the activation of apoptosis and are accomplished through the downstream signalling of pro-apoptotic (Bax) and anti-apoptotic (Bcl-2) proteins. Earlier works reported overexpression of inflammatory cytokines, TNFα, IL-6, IL-1β and caspases in both experimental humans and animals with INH-induced hepatic injury[53]. RFP activates cytokine-induced release of pro-inflammatory mediators, including IL-8 and nitric oxide, in the liver cell line[54].

Figure 9 shows that INH- and RFP-treated rats (Group II) had significantly higher cytokine levels (TNFα, IL-6, IL-8, and IL-1β) than the control (Group I) ($p < 0.0001$). A remarkable reduction in these inflammatory cytokine markers is observed for the *P. acidus* extract, 400 mg/kg dose, which clearly indicates that the extract has occluded the liberation of inflammatory cytokines. No notable difference in cytokine levels in the extract (200 mg/kg) compared to the INH and RFP groups was found. The standard group has shown a distinctive decrease in these markers.

3.6.5 Histopathology of the Liver

For histopathological studies, three different stains were used for staining the liver tissues. Firstly, Figure 10 (i) displays the Hematoxylin and eosin-stained liver sections where (A) the control group indicated normal liver architectural characteristics with networks of cords of liver cells, thickness (1-2 cells), diverging from Central Veins (CV) and separated from one another by constricted sinusoids. Bile ducts and branches of the Portal Veins (PV) can also be observed. INH and RFP group (B) produced the most liver injury. Many regions of Mononuclear Cellular Infiltration (MCI) are found amidst the liver cells, around the central vein, or in the portal region, due to disturbances in the liver architecture. (C) The low dose of bark extract demonstrated noticeable hepatocellular degradation. Several cells are observed with hyper-eosinophilic cytoplasm, decreased cytoplasmic granularity and dark, irregular nuclei. Dilated sinusoids are lined by several Kupffer cells. (D) The high-dose bark extract showed good protection of liver cells, with pale, large nuclei and some binucleated cells. Regions of Mononuclear Cellular Infiltration (MCI) are still recognisable within the cells or in the portal vein. Furthermore, the hepatocytes of the standard group (E) appear to be more/less normal, with minor eosinophilic granular cytoplasm and large central vesicular nuclei with distinct nucleoli. Besides, several binucleated liver cells can be observed. Regions of mononuclear cellular infiltration and many Kupffer cells can also be noticed. Secondly, the Toluidine-O-blue staining of liver sections of different groups is demonstrated in Figure 10 (ii). Control (A) had normal liver architectural characteristics with minute unsaturated lipid droplets. In B and C, fatty degeneration, degenerative cells, mast cell infiltration and vacuolisation in hepatocytes were

noticed in the (B) INH- and RFP administered and (C) 200 mg/kg bark extract groups, respectively. Similarly, the 400 mg/kg extract (D) has protected the cells of the liver well from damage. Mast cell infiltration, unsaturated fatty acid lipid droplets and dilation in sinusoids have been reduced. The silymarin (E) group has displayed similar characteristics to the control (A). The third stain used for staining the liver tissues was Masson's trichrome stain Figure 10 (iii). In the control group (A), the liver's normal characteristic features are observed, with collagen fibre deposition in and around the area of the portal vein, as shown by arrows. INH and RFP (B) increased the amount of collagen fibre deposits in the portal area (PV) and around the Central Veins (CV); fibrosis formation can be observed (shown with arrows). Extract low dose (C) displays a moderate reduction in collagen fibre deposits. The high-dose extract exhibited reduced collagen fibre deposits in the liver parenchyma, in contrast to the control group. Silymarin (E) indicated the slightest collagen expression in the surroundings of the central veins.

4. Conclusion

This research study found that *P. acidus* bark provides protection from antitubercular medication and prevents liver toxicity. *P. acidus* bark offers significant antioxidants for the prevention of hepatocytes from oxidative stress, which leads to apoptosis and necrosis, produced by isoniazid and rifampicin in a dose-dependent manner. Therefore, *P. acidus* bark can be considered a novel and effective agent in the protection and amelioration of liver damage when administered along with the antitubercular agents.

5. Acknowledgements

I would like to express my heartfelt gratitude to Deccan School of Pharmacy for permitting me to conduct the animal study at their esteemed institution. I am also deeply grateful to Dr. Vijay Kumar, SIF, Vellore Institute of Technology, for his invaluable support in our studies.

6. References

1. Zhuang X, Li L, Liu T, Zhang R, Yang P, Wang X, *et al*. Mechanisms of isoniazid and rifampicin-induced liver injury and the effects of natural medicinal ingredients: A review. Front Pharmacol. 2022; 13:1037814. https://doi.org/10.3389/fphar.2022.1037814 PMID:36299895 PMCID:PMC9589499
2. Mujahid M, Hussain T, Siddiqui HH, Hussain A. Evaluation of hepatoprotective potential of *Erythrina indica* leaves against antitubercular drugs-induced hepatotoxicity in experimental rats. J Ayurveda Integr Med. 2017; 8:7-12. https://doi.org/10.1016/j.jaim.2016.10.005 PMID:27916487 PMCID:PMC5377476
3. Choijamts G, Batsyren C, Orkhon B, Otgontyr, Narantstsetseg D, Oyunerdene X, *et al*. Role of Liv.52 DS tablets as a hepatoprotective agent in tuberculosis patients receiving antitubercular drugs: A double-blind, placebo-controlled study. J Liver Clin Res. 2018; 5:1042-50. https://doi.org/10.47739/2379-0830/1042
4. Khan FY. Clinical pattern of tuberculous adenitis in Qatar: Experience with 35 patients. Scand J Infect Dis. 2009; 41:128-34. https://doi.org/10.1080/00365540802578991 PMID:19012183
5. Devarbhavi H, Singh R, Patil M, Sheth K, Adarsh CK, Balaraju G. Outcome and determinants of mortality in 269 patients with combination anti-tuberculosis drug-induced liver injury. J Gastroenterol Hepatol. 2013; 28(1):161-167. https://doi.org/10.1111/j.1440-1746.2012.07279.x PMID:23020522
6. Singh M, Sasi P, Gupta VH, Rai G, Amarapurkar DN, Wangikar PP. Protective effect of curcumin, silymarin and N-acetylcysteine on antitubercular drug-induced hepatotoxicity assessed in an *in vitro* model. Hum Exp Toxicol. 2012; 31:788-797. https://doi.org/10.1177/0960327111433901 PMID:22318308.
7. Jain NK, Singhai AK. Protective effects of *Phyllanthus acidus* (L.) Skeels leaf extracts on acetaminophen- and thioacetamide-induced hepatic injuries in Wistar rats. Asian Pac J Trop Med. 2011; 4(6):470-474. https://doi.org/10.1016/S1995-7645(11)60128-4 PMID:21771701
8. Lim TK. Edible medicinal and non-medicinal plants. Vol. 4, Fruits. Dordrecht: Springer; 2012. p. 256-266. https://doi.org/10.1007/978-94-007-4053-2
9. Tropical Plants Database. *Phyllanthus acidus*. Ken fern. 2014 [cited 2019 Jan 31]. Available from: http://tropical.theferns.info/viewtropical.php?id=Phyllanthus+acidus
10. Lemmens RHMJ, Buntapraphatsara N, Padua de LS. Plant resources of South-East Asia No. 12: medicinal and poisonous plants. Indonesia: Prosea Foundation; 1999. p. 386-387.
11. Morton JF. Otaheite gooseberry. In: Fruits of warm climates. Miami (FL); 1987. p. 217-219.
12. Tan SP, Tan EN, Lim QY, *et al*. *Phyllanthus acidus* (L.) Skeels: A review of its traditional uses, phytochemistry, and pharmacological properties. J Ethnopharmacol. 2020; 253:112610. https://doi.org/10.1016/j.jep.2020.112610 PMID:31991202

13. Sengupta P, Mukhopadhyay J. Terpenoids and related compounds—VII: Triterpenoids of *Phyllanthus acidus* Skeels. Phytochemistry. 1966; 5(3):531-534. https://doi.org/10.1016/S0031-9422(00)82169-X
14. Gu C, Yin AP, Yuan HY, Yang K, Luo J, Zhan YJ, *et al*. New anti-HBV norbisabolane sesquiterpenes from *Phyllanthus acidus*. Fitoterapia. 2019; 137:104151. https://doi.org/10.1016/j.fitote.2019.04.006 PMID:30999024
15. Shilali K, Ramachandra YL, Rajesh KP, Swamy BEK. Assessing the antioxidant potential of *Phyllanthus acidus* bark extracts. Int J Pharm Pharm Sci. 2014; 6(6):522-531.
16. Biswas SK, Chowdhury A, Das J, Karmakar UK, Shill MC, Raihan SZ. Assessment of cytotoxicity, antibacterial activity and phytochemical screening of ethanol extract of *Phyllanthus acidus* bark. J Appl Pharm Sci, 2011; 1(6):112-114.
17. Ferguson NM. A textbook of pharmacognosy. New Delhi: Macmillan; 1956. p. 191.
18. Singleton VL, Rossi JA. Colorimetry of total phenolics with phosphomolybdic-phosphotungstic acid reagents. Am J Enol Vitic. 1965; 16:144-158. https://doi.org/10.5344/ajev.1965.16.3.144
19. Rahman MM, Habib MR, Hasan R, Sayeed MA. Antibacterial, cytotoxic and antioxidant potential of methanolic extract of *Phyllanthus acidus*. Int J Drug Dev Res. 2011; 3:154-161.
20. Inamdar S, Ahmad M, Tazneem B, Hashmi S, Kulkarni B, Aldhabi BM, *et al*. Molecular docking analysis of *Ficus religiosa* fruit extracts with HMG-CoA reductase inhibitors and anti-hyperlipidemic effects in albino Wistar rats. Bioact Carbohydr Diet Fibre. 2024; 32:100429. https://doi.org/10.1016/j.bcdf.2024.100429
21. Kanakal MM, Abbas SA, Khan A, Sultana S, Fatima H, Tabasssum R, *et al*. Using Quality by Design tools to study gel formulation from *Brassica juncea* leaves and conducting its *in vitro*, *in vivo*, molecular docking, and ADMET analyses. Anti Inflamm Anti Allergy Agents Med Chem. 2024; 23(3):187-204. https://doi.org/10.2174/0118715230309053240718122527 PMID:39082166
22. Khan A, Bachi T, Fatima H, Irfan M, Khan MM, Fatima M, *et al*. Central composite design tool application for optimizing methanolic leaves extract of *Ceiba pentandra* ethosome suspension gel with *in silico*, *in vitro*, and *in vivo* anti-inflammatory effects. Curr Bioact Compd. 2025; 21:e15734072354861. https://doi.org/10.2174/0115734072354861250526073734
23. Sulukoğlu EK, Günaydın Ş, Kalın ŞN, Altay A, Budak H. Diffractaic acid exerts anti-cancer effects on hepatocellular carcinoma HepG2 cells by inducing apoptosis and suppressing migration through targeting thioredoxin reductase 1. Naunyn Schmiedebergs Arch Pharmacol. 2024; 397(8):5745-5755. https://doi.org/10.1007/s00210-024-02980-5 PMID:38308689 PMCID:PMC11329542
24. Vuran NE, Kartal DI, Çelik I. Antiproliferative activity of *Malus sylvestris* Miller against HepG2 cell line with antioxidant properties and phenolic composition. Turk J Biochem. 2023; 48(3):272-281. https://doi.org/10.1515/tjb-2022-0186
25. Cakil YD, Ozunal ZGO, Kayali DG, Aktas RG, Saglam E, *et al*. Anti-proliferative effects of paroxetine alone or in combination with sorafenib in HepG2 cells. Braz J Pharm Sci. 2022; 58:e201148. https://doi.org/10.1590/s2175-97902022e201148
26. Djabir YY, Adnan J, Amaliah N, Ramli N, Sartini S, Mamada SS, *et al*. Roselle (*Hibiscus sabdariffa* L.) calyx water extract ameliorates isoniazid- and rifampicin-induced liver and renal injuries in rats. J Herbmed Pharmacol. 2021; 10(3):296-303. https://doi.org/10.34172/jhp.2021.34
27. Su Q, Kuang W, Hao W, Liang J, Wu L, Tang C, *et al*. Antituberculosis drugs (rifampicin and isoniazid) induce liver injury by regulating NLRP3 inflammasomes. Mediators Inflamm. 2021; 2021:8086253. https://doi.org/10.1155/2021/8086253 PMID:33688304 PMCID:PMC7914095
28. Urfi MK, Mujahid, Rahman MA, Rahman A. Role of *Tamarix gallica* leaves extract in liver injury induced by rifampicin plus isoniazid in Sprague-Dawley rats. J Diet Suppl. 2018; 15(1):24-33. https://doi.org/10.1080/19390211.2017.1310783 PMID:28459346
29. Pant R, Irchhaiya R, Rao CV. Phytochemical and pharmacological evaluation of *Carthamus tinctorius* leaves. J Drug Deliv Ther. 2019; 9(4 Suppl):285-294. https://doi.org/10.22270/jddt.v9i4-s.3277
30. Lowry OH, Rosebrough NJ, Farr AL, Randall RJ. Protein measurement with the Folin phenol reagent. J Biol Chem. 1951; 193:265-275. https://doi.org/10.1016/S0021-9258(19)52451-6 PMID:14907713 PMCID:PMC11896512
31. Islam F, Zia S, Sayeed I, Zafar KS, Ahmad AS. Selenium-induced alteration of lipids, lipid peroxidation, and thiol group in circadian rhythm centers of rat. Biol Trace Elem Res. 2002; 90(1-3):203-214. https://doi.org/10.1385/BTER:90:1-3:203 PMID:12666835
32. Jollow DJ, Mitchell JR, Zampaglione N, Gillette JR. Bromobenzene-induced liver necrosis: Protective role of glutathione and evidence for 3,4-bromobenzene oxide as the hepatotoxic intermediate. Pharmacology. 1974;1 1(3):151-169. https://doi.org/10.1159/000136485 PMID:4831804
33. Clariborne A. Catalase activity. In: Greenwald RA, editor. CRC handbook of methods for oxygen radical research. Boca Raton (FL): CRC Press; 1985. p. 283-284.
34. Marklund S, Marklund G. Involvement of superoxide anion radical in the autoxidation of pyrogallol and a convenient assay for superoxide dismutase.

Eur J Biochem. 1974; 47(3):469-474. https://doi.org/10.1111/j.1432-1033.1974.tb03714.x PMID:4215654 PMCID:PMC10542938

35. Gong G, Yuan LB, Hu L, Wu W, Yin L, Hou J, *et al*. Glycyrrhizin attenuates rat ischemic spinal cord injury by suppressing inflammatory cytokines and HMGB1. Acta Pharmacol Sin. 2012; 33:11-18. https://doi.org/10.1038/aps.2011.151 PMID:22158106 PMCID:PMC4010273
36. Tag HM. Hepatoprotective effect of mulberry (*Morus nigra*) leaves extract against methotrexate-induced hepatotoxicity in male albino rats. BMC Complement Altern Med. 2015; 15:252. https://doi.org/10.1186/s12906-015-0744-y PMID:26209437 PMCID:PMC4514987
37. Siddiqui T, Khan MU, Sharma V, Gupta K. Terpenoids in essential oils: chemistry, classification, and potential impact on human health and industry. Phytomedicine Plus. 2024; 4(2):100549. https://doi.org/10.1016/j.phyplu.2024.100549
38. Tungmunnithum D, Thongboonyou A, Pholboon A, *et al*. Flavonoids and other phenolic compounds from medicinal plants for pharmaceutical and medical aspects: an overview. Medicines. 2018; 5(3):93. https://doi.org/10.3390/medicines5030093 PMID:30149600
39. Allameh A, Niayesh-Mehr R, Aliarab A, Sebastiani G, Pantopoulos K. Oxidative stress in liver pathophysiology and disease. Antioxidants. 2023; 12(9):1653. https://doi.org/10.3390/antiox12091653 PMID:37759956 PMCID:PMC10525124
40. Hwang KA, Hwang YJ, Song J. Antioxidant activities and oxidative stress inhibitory effects of ethanol extracts from *Cornus officinalis* on RAW 264.7 cells. BMC Complement Altern Med. 2016; 16:196. https://doi.org/10.1186/s12906-016-1172-3 PMID:27391600 PMCID:PMC4939040
41. Bhalodia N, Nariya P, Shukla V, Acharya R. *In vitro* antioxidant activity of hydroalcoholic extract from the fruit pulp of *Cassia fistula* Linn. AYU. 2013; 34(2):209-214. https://doi.org/10.4103/0974-8520.119684 PMID:24250133 PMCID:PMC3821253
42. Das R, Paul P, Mukherjee K, Mitra S, Singh U, Banerjee ER. Anti-oxiflammatory profile of date extracts (*Phoenix sylvestris*). Biomed Res Ther. 2015; 2(6):297-317. https://doi.org/10.15419/bmrat.v2i06.53
43. Gomathi D, Kalaiselvi M, Ravikumar G, Devaki K, Uma C. GC-MS analysis of bioactive compounds from whole plant ethanolic extract of *Evolvulus alsinoides.* J Food Sci Technol. 2015; 52(2):1212-1217. https://doi.org/10.1007/s13197-013-1105-9 PMID:25694742 PMCID:PMC4325072
44. Agu PC, Afiukwa CA, Orji OU, *et al*. Molecular docking as a tool for discovery of molecular targets of nutraceuticals in disease management. Sci Rep. 2023; 13:13398. https://doi.org/10.1038/s41598-023-40160-2 PMID:37592012 PMCID:PMC10435576
45. Huyck L, Ampe C, Van Troys M. The XTT cell proliferation assay applied to cell layers embedded in three-dimensional matrix. Assay Drug Dev Technol. 2012; 10(4):382-392. https://doi.org/10.1089/adt.2011.391 PMID:22574651; PMCID:PMC3419859
46. Koban I, Matthes R, Hübner NO, Welk A, Sietmann R, Lademann J, *et al*. XTT assay of *ex vivo* saliva biofilms to test antimicrobial influences. GMS Krankenhhyg Interdiszip. 2012; 7(1):Doc06. https://doi.org/10.3205/dgkh000190
47. Wali AF, Avula B, Ali Z, Khan IA, Mushtaq A, Rehman MU, *et al*. Antioxidant and hepatoprotective potential and chemical profiling of propolis ethanolic extract from Kashmir Himalaya using UHPLC-DAD-QToF-MS. Biomed Res Int. 2015; 2015:393462. https://doi.org/10.1155/2015/393462 PMID:26539487 PMCID:PMC4619790
48. Muriel P. Role of free radicals in liver diseases. Hepatol Int. 2009; 3(4):526-536. https://doi.org/10.1007/s12072-009-9158-6 PMID:19941170 PMCID:PMC2790593
49. Kale BP, Kothekar MA, Tayade HP, Jaju JB, Mateenuddin M. Effect of aqueous extract of *Azadirachta indica* leaves on hepatotoxicity induced by antitubercular drugs in rats. Indian J Pharmacol. 2003; 35:177-180.
50. Sodhi CP, Rana SV, Mehta SK, K. Vaiphei, S. Attari, Mehta S. Study of oxidative stress in isoniazid-rifampicin-induced hepatic injury in young rats. Drug Chem Toxicol. 1997; 20:255-269. https://doi.org/10.3109/01480549709003881 PMID:9292280
51. Onyema OO, Farombi EO, Emerole GO, Ukoha AI, Onyeze GO. Effect of vitamin E on monosodium glutamate-induced hepatotoxicity and oxidative stress in rats. Indian J Biochem Biophys. 2006; 43(1):20-24 PMID:16955747
52. Ohta Y, Kongo-Nishimura M, Imai Y, Matsura T, Kitagawa A, Yamada K. α-Tocopherol protects against α-naphthylisothiocyanate-induced hepatotoxicity in rats less effectively than melatonin. Chem Biol Interact. 2006; 161(2):115-124. https://doi.org/10.1016/j.cbi.2006.03.006 PMID:16626673
53. Anwer T, Alruwaili MN, Alshahrani S, Alqahtani SS, Jali A, Ahmed RA, *et al*. Hepatoprotective potential of diosmin against isoniazid- and rifampin-induced hepatotoxicity in Wistar rats. Hum Exp Toxicol. 2023; 42. https://doi.org/10.1177/09603271221149199 PMID:36592122
54. Yuhas Y, Berent E, Ashkenazi S. Effect of rifampin on production of inflammatory mediators in HepG2 liver epithelial cells. Antimicrob Agents Chemother. 2011; 55:5541-5546. https://doi.org/10.1128/AAC.05149-11 PMID:21930886 PMCID:PMC3232822

Author Contribution

Humaira Fatima: Concepts, Definition of intellectual content, Literature search, Experimental studies, Data analysis, Statistical analysis, Manuscript preparation. Rokeya Sultana: Concepts, Design, Manuscript editing, Manuscript review. S. Roshan: Design, Experimental studies, Data acquisition, Data analysis, Statistical analysis, Manuscript editing, Manuscript review. All authors have read and agreed to the published version of the manuscript.